ELSEVIER

www.elsevier.nl/locate/jorganchem

Journal of Organometallic Chemistry 586 (1999) 176–183

Journal of Organometallic Chemistry

Paramagnetic ruthenium(III) *ortho*-metallated complexes. Synthesis, spectroscopic and redox properties

Pradip Munshi, Ramapati Samanta, Goutam Kumar Lahiri *

Department of Chemistry, Indian Institute of Technology, Bombay, Powai, Mumbai 400076, India

Received 3 March 1999; received in revised form 5 May 1999

Abstract

The reaction of $(CS)Cl(PPh_3)_2Ru^{II}$ $(\mu\text{-}Cl)_2$ Ru^{II} $(PPh_3)_2Cl(CS)$, **A** with the phenolic Schiff base ligands *o*-$(OH)C_6H_4C(H)$=N-$C_6H_4(R)$, (R = *p*-OMe, Me, H, Cl, NO_2; H_2L^1–H_2L^5) in methanol under aerobic conditions afforded the complexes $Ru^{III}(HL)_2(PPh_3)Cl$, **1** and $Ru^{III}(L)(PPh_3)(CH_3OH)Cl$, **2**. In complexes **1** both the ligands (HL^-) are bound to the metal center at the deprotonated phenolic oxygen and azomethine nitrogen and in the complexes **2** the L^{2-} is in tridentate C,N,O mode where cyclometallation takes place from the *ortho* carbon atom of the amine fragment of H_2L. During the reaction the metal ion is oxidized from the starting Ru^{II} in **A** to Ru^{III} in the products **1** and **2**. The complexes (**1** and **2**) are nonconducting and behave as one-electron paramagnets. Complexes display rhombic EPR spectra that have been analyzed to furnish values of axial ($\triangle$) and rhombic (V) distortion parameters as well as energies of the two expected ligand field transitions (v_1 and v_2) within the t_2 shell. One of the transitions (v_2) has been observed in the predicted region. The complexes exhibit moderately strong ligand-to-metal charge-transfer transition in the visible region and intraligand transitions in the UV region. The complexes are electroactive and show ruthenium (IV)–ruthenium(III) ($E_{1/2}$, 0.75–0.88 V vs. Ag/AgCl) and ruthenium(III)–ruthenium(II) ($E_{1/2}$, -0.42 to -0.59 V) couples. The $E_{1/2}$ values vary linearly with the Hammett constant of the substituents R. The role of coordination of phenolato function in stabilizing the unusual paramagnetic ruthenium(III) oxidation state in the complexes **2** is noted.

Keywords: Ruthenuim(III); *Ortho*-metallation; Schiff base; Paramagnetic; EPR

1. Introduction

Ruthenium cyclometallated complexes are virtually restricted to the diamagnetic bivalent ruthenium(II) oxidation state inspite of the fact that the variable valence property pervades the chemistry of ruthenium [1–17]. Although the coordination chemistry of trivalent ruthenium(III) has been developed tremendously in recent years, the corresponding paramagnetic ruthenium(III) organometallic species are rare [18]. Only a few authentic paramagnetic trivalent ruthenium organometallic complexes are known up to now [19–34].

The present work originates from our interest to generate a new class of paramagnetic ruthenium(III) cyclometallated complexes. In this article we would like to report the syntheses of a group of such complexes of the type $Ru^{III}(C, N, O)(PPh_3)(Cl)(CH_3OH)$ (**2**). The complexes **2** are formed along with the noncyclometallated complex of the type $Ru^{III}(O,N)_2(PPh_3)Cl$ (**1**) via the cleavage of bridging chloride groups of the μ-dichlorodiruthenium starting complex (**A**) in the presence of phenolic Schiff base ligand H_2L. Herein the synthesis, spectroscopic characterization and electron-transfer properties of the complexes (**1** and **2**) have been described.

2. Results and discussion

2.1. Synthesis and characterization of the complexes

The reaction of phenolic Schiff base ligand H_2L with the dichloro bridged diruthenium starting complex **A** in a ratio of 5:1 in boiling methanol for 5 h results in a

* Corresponding author. Fax: +91-22-5783480.
E-mail address: lahiri@ether.chem.iitb.ernet.in (G. Kumar Lahiri)

0022-328X/99/$ - see front matter
PII: S0022-328X(99)00261-2

green solution. Chromatographic purification of the green solution on a silica gel column yield yellowish green colored cyclometallated complex **2** along with the bluish green noncyclometallated complex **1** in the pure solid state (Scheme 1).

The formations of complexes **1** and **2** involve the cleavage of μ-chloro bonds of **A** followed by the replacement of one phosphine, thiocarbonyl (CS) and terminal chloride from the resultant monomeric ruthenium species by two (HL^-) and one L^{2-}, respectively. Here in the course of the reaction one metal–carbon σ-bond has been formed in **2** from the pendant phenyl ring of the coordinated ligand L^{2-}. During this conversion process the ruthenium ion is oxidized from its starting bivalent state in **A** to the trivalent state in both the products **1** and **2**. Since the reaction (Scheme 1) takes place preferentially under atmospheric conditions, the oxygen in air may be responsible for the metal oxidation (see later). It may be noted that the cleavage of μ-chloro bonds of **A** and the partial or full replacement of PPh_3, CS and terminal Cl^- by the azopyridine, 2-2′-bipyridine or phenanthroline ligands have been observed recently [35,36]. The formation of four and five membered stable ruthenium–carbon σ-bond from the pendant phenyl ring of azo and imine based ligands have been documented in the literature [15,16,31, 33,34,37].

To generalize the reaction in Scheme 1 five substituted ligands (abbreviated as H_2L^1–H_2L^5) have been used. The conversion of isolated complex **1** to **2** in methanol solution and the transformation of isolated complex **2** to **1** in the presence of excess H_2L did not take place even under heating condition. However, the methanol group of **2** can be replaced by other monodentate ligands such as carbon monoxide, triphenylphosphine or pyridine.

The microanalytical data of the complexes are in good agreement with the calculated values (Table 1). The conductivity measurements of the complexes in acetonitrile, dimethylformamide and methanol indicate that all the complexes (**1** and **2**) are electrically nonconducting.

The FAB mass spectra of two representative complexes of each class (**1a**, **1b,** and **2a**, **2b**) were recorded. The representative spectra are shown in Fig. 1. The maximum peaks are observed at m/z, 790, 819, 626, 639 for the complexes **1a**, **1b**, **2a** and **2b**, respectively, which match well with the corresponding calculated masses (calculated molecular weight: **1a**, 790.6; **1b**, 818.6; **2a**, 625.6; **2b**, 639.6).

Thermogravimetric analyses (TGA) of one representative complex of each class (**1d** and **2d**) were studied. The complexes **1d** and **2d** show three- and four-step decomposition patterns respectively. The three successive decompositions take place for **1d** near 175, 288 and 440°C corresponding to the weight loss of one chlorine, one phosphine and two ligands (HL^-), respectively. The TGA of complex **2d** shows one additional decomposition step due to the coordinated methanol. The four successive decompositions take place at 85, 170, 290 and 450°C corresponding to the weight loss of one each CH_3OH, Cl^-, PPh_3 and L^{2-} respectively. The differential thermal analyses (DTA) of the complexes (**1d** and **2d**) further confirm the above decomposition patterns. It display successive three and four exothermic peaks for **1d** and **2d**, respectively, as expected.

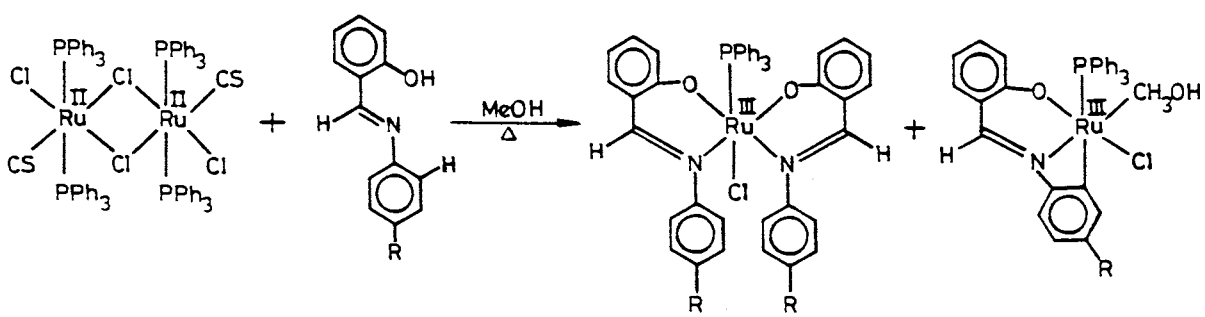

Scheme 1.

Table 1
Microanalytical, selected infrared and electronic spectral data

Compound	Elemental analysis (%) [a]			IR [b], ν_{max} (cm^{-1})		Electronic spectral data [c]
	C	H	N	C=N	Ru–Cl	λ (nm) (ε, $dm^3\ mol^{-1}\ cm^{-1}$)
1a	65.77(65.81)	4.51(4.54)	3.32(3.41)	1595	330	617(6810), 359(56370), 304(67822)
1b	67.28(67.11)	4.60(4.63)	3.31(3.48)	1597	335	622(5972), 354(41818), 304(48770)
1c	66.85(66.79)	4.55(4.46)	3.47(3.54)	1597	337	619(4545), 345(34793), 304(34839)
1d	63.91(64.00)	4.18(4.15)	3.49(3.39)	1594	337	651(2082), 346(11112), 301(15294)
1e	63.31(63.19)	4.05(4.09)	5.11(5.02)	1598	335	690(8222), 345(23019), 304(23535)
2a	60.19(60.32)	4.67(4.75)	2.22(2.13)	1596	340	621(3950), 404(10577), 304(21056)
2b	61.70(61.82)	4.81(4.87)	2.02(2.18)	1597	342	635(5509), 369(33779), 304(56158)
2c	61.37(61.29)	4.72(4.66)	2.38(2.23)	1598	339	686(4581), 346(21695), 301(24582)
2d	58.23(58.10)	4.29(4.26)	2.25(2.12)	1594	337	690(4004), 345(19304), 304(18608)
2e	57.05(57.19)	4.18(4.20)	4.31(4.17)	1595	339	674(3544), 359(40835), 305(43589)

[a] Calculated values are in parentheses.
[b] In KBr disk.
[c] In dichloromethane.

All our attempts to grow suitable single crystals for X-ray characterization of **2** have failed. However, elemental analysis and all other physical data are in agreement with the gross formulation of **2**.

2.2. IR, UV–vis and NMR spectra

Selective IR frequencies are listed in Table 1. The $\nu_{C=N}$ stretching frequency of the free ligands (H_2L) appears near 1650 cm^{-1}, which has been shifted to $\sim$1590 cm^{-1} in the complexes **1** and **2** in accordance with the coordination of the azomethine function to the metal ion [38]. Phosphine vibrations for the complexes appear around 700 and 520 cm^{-1} [39]. A sharp band near 340 cm^{-1} has been observed for all the complexes due to ν_{Ru-Cl} stretching frequency.

The complexes (**1** and **2**) display one moderately intense band in the region 600–700 nm (Table 1, Fig. 2). The position and intensity of the bands are sensitive to the nature of the substituents present in the ligands (Table 1). The observed visible-region band is believed to represent ligand-to-matal charge-transfer (LMCT) transition as is expected for low-spin ruthenium(III) complexes of unsaturated ligands [40–42]. In the UV region the complexes systematically exhibit two very intense bands (Table 1), possibly due to ligand based transitions [35].

^{1}H-NMR spectra of the complexes (**1** and **2**) in $CDCl_3$ solvent display very broad signals due to the paramagnetic nature of the complexes, which has precluded the identification of the individual protons of the complexes. However, a direct comparison of the observed integration of the aliphatic proton signals with that of the aromatic region signals reveals the presence of the calculated number of aromatic protons.

^{31}P-NMR spectra of both the complexes in $CDCl_3$ solvent display one sharp signal near 30 ppm.

2.3. Magnetism, EPR and near-IR spectra

The complexes (**1** and **2**) are uniformly paramagnetic with magnetic moments correspond to one unpaired electron at 298 K (low-spin Ru^{III}, t_{2g}^5). The data are set out in Table 2. The X-band EPR spectra of the complexes in glassy 1:1 chloroform–toluene solution (77 K) is rhombic in nature with three distinct signals. The representative spectra are shown in Fig. 3 and the g values are listed in Table 2.

The theory of EPR spectra of distorted octahedral low-spin d^5 (idealized t_{2g}^5 ground term $^2T_{2g}$) complexes is documented in the literature [31,33–35,37–39,42–48]. The distortion of the pseudooctahedral complexes can be expressed as the sum of axial ($\triangle$) and rhombic (V) components. The t_2 orbital consists of the components t_2^0 (xy), t_2^+ (xz) and t_2^- (yz). The degeneracy of the t_2 orbital is partially removed by axial distortion ($\triangle$), which places t_2^0 (b) above t_2^+/t_2^- (e). The superimposed rhombic distortion (V) then splits (e) further into t_2^+ and t_2^-.

The analysis of the EPR spectrum using the g-tensor theory of low-spin d^5 ions provides the distortion parameters ($\triangle$ and V) of the complex and energies of two ligand field transitions (ν_1 and ν_2) that arise due to optical transitions from ground to upper Kramers doublets [31].

The EPR experiments provide only the absolute g values and so neither their signs nor the correspondence of g_1, g_2 or g_3 to g_x, g_y or g_z are known. There are 48 possible combinations depending on the labeling of x, y, z and signs chosen for the experimentally observed EPR g values. In the present complexes we have considered the particular combination where g_1 and g_2 are negative, g_3 is positive and the order of magnitude $g_1 > g_2 > g_3$. This particular combination results in a reasonable value of k (orbital reduction factor < 1.0,

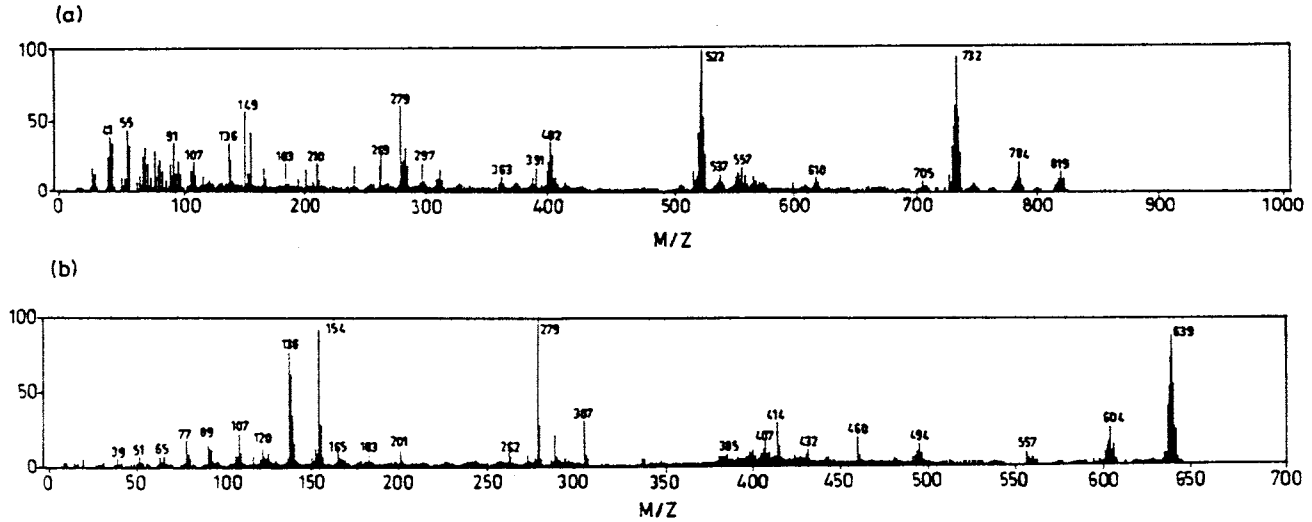

Fig. 1. FAB mass spectra of (a) $Ru^{III}(HL^2)_2(PPh_3)Cl$, **1b** and $Ru^{III}(L^2)(PPh_3)(CH_3OH)Cl$, **2b**.

Table 2). The value of k for all other combinations of g parameters does not satisfy the limit of k ($k < 1.0$), and is therefore not acceptable. The computed values of axial distortion ($\triangle$), rhombic distortion (V) and the two ligand field transitions (ν_1 and ν_2) for the complexes are listed in Table 2. The value for the spin–orbit coupling constant of ruthenium(III) is taken as 1000 cm^{-1} [42].

The calculated values of ν_1 and ν_2 are observed near 4000 and 9000 cm^{-1}, respectively (Table 2). Experimentally by near-IR spectra the ν_2 band is observed in the expected positions (Table 2). In view of the approximations involved in the theory, the agreement between the experimental and theoretical ν_2 values (Table 2) is excellent. Due to the instrumental wavelength scan limitation (maximum up to 2200 nm) it has not been possible to check the ν_1 band properly. However, the increase of absorption starting further from 2000 nm for all the complexes gives clear indication of the presence of ν_1 band near the calculated region. In general, here the axial distortion is 20–25% more than the rhombic distortion. The complexes **1** and **2** thus behave as model ruthenium(III) complexes possessing rhombic symmetry.

2.4. Redox properties

The redox properties of the complexes have been studied in dichloromethane solution by cyclic voltammetry and differential pulse voltammetry using a platinum working electrode. The complexes (**1** and **2**) are electroactive with respective to the metal center only and display the same two redox processes in the potential range ± 1.5V vs. Ag/AgCl. Representative voltammograms are shown in Fig. 4 and the potential data are listed in Table 3.

The complexes of type **1** exhibit one quasi-reversible oxidative couple in the range 0.78–0.88 V and one quasi-reversible reductive response in the range $-0.48 \rightarrow -0.58$ V [the difference between the oxidation and reduction peak potentials (ΔE_p) is observed to be in the range 90–100 mV]. The one-electron nature of the oxidative couple at the positive side of Ag/AgCl is established with the help of constant potential coulometry (Table 3). The oxidized complexes $\mathbf{1}^+$ display cyclic voltammograms that are superposable to those of the corresponding starting trivalent complexes **1**, suggesting that the oxidation process here may be stereoretentive in nature. Thus the oxidation process is assigned to ruthenium(III)–ruthenium(IV) couple (Eq. (1)).

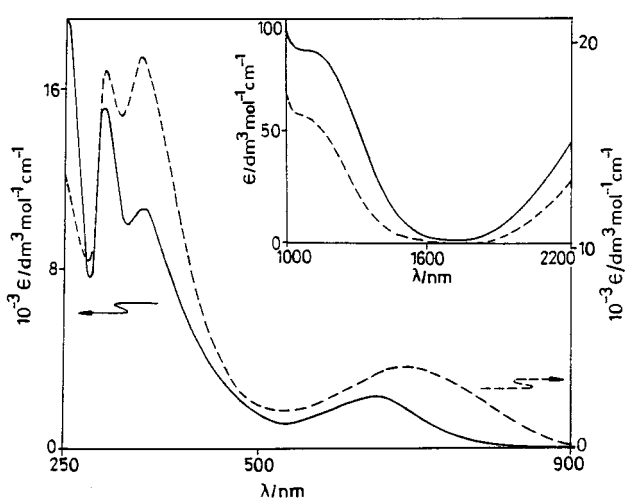

Fig. 2. Electronic spectra of $Ru^{III}(HL^4)_2(PPh_3)Cl$, **1d** (—) and $Ru^{III}(L^4)(PPh_3)(CH_3OH)Cl$, **2d** (---) in dichloromethane. Inset: electronic spectra of **1d** (—) and **2d** (---) in the range 2200–1000 nm.

Table 2
Bulk magnetic moments [a], g values [b], distortion parameters and transition energies

Compound	μ_{eff}, μ_B	g_1	g_2	g_3	k	Δ (cm^{-1})	V (cm^{-1})	ν_1 (cm^{-1})	ν_2 (cm^{-1})	$\nu_{2\ (obs)}$ (cm^{-1})
1a	1.97	−2.356	−2.081	1.874	0.648	6073	5135	3647	8819	8342 (110) [c]
1b	1.99	−2.370	−2.099	1.897	0.741	6834	5832	4043	9909	(9471)(100) [c]
1c	1.99	−2.339	−2.108	1.896	0.699	6408	4798	4127	8978	(8549)(90) [c]
1d	1.95	−2.371	−2.107	1.891	0.735	6482	5242	3987	9271	(8988)(85) [c]
1e	1.93	−2.369	−2.100	1.903	0.759	7091	6111	4157	10299	(9902)(80) [c]
2a	1.95	−2.339	−2.067	1.852	0.579	5462	4464	3384	7892	(8100)(67) [c]
2b	1.94	−2.352	−2.072	1.900	0.691	7277	6876	3969	10864	(10410)(55) [c]
2c	1.95	−2.325	−2.082	1.887	0.628	6267	5067	3864	8974	(8640)(68) [c]
2d	1.99	−2.354	−2.087	1.882	0.667	6259	5231	3779	9048	(9530)(56) [c]
2e	1.96	−2.352	−2.100	1.881	0.675	6053	4700	3834	8583	(9100)(72) [c]

[a] In solid state at 298 K.
[b] In 1:1 chloroform–toluene glass at 77 K.
[c] Intensity ($dm^3\ mol^{-1}\ cm^{-1}$) values are given in parantheses.

$$[Ru^{IV}(N,O)_2(PPh_3)Cl]^+ + e^- \rightleftharpoons [Ru^{III}(N,O)_2(PPh_3)Cl] \quad (1)$$
$$\mathbf{1}^+ \qquad\qquad \mathbf{1}$$

Although the red–brown colored tetravalent ruthenium(IV) congener of **1** can be developed in solution by bulk electrolysis, the $\mathbf{1}^+$ species is not stable enough to be isolated in the pure solid state at room temperature.

The one-electron nature of the reduction couple at the negative side of Ag/AgCl is confirmed by a direct comparison of the differential pulse current height of this response with that of the previous one-electron $Ru^{III} \rightarrow Ru^{IV}$ process occurring at the positive side of Ag/AgCl (Eq. (1)). The coulometric reduction of the complexes **1** at a potential ~ 200 mV negative to the E_{pc} of the corresponding reduction couple showed very small coulomb count indicating that the reduced species $\mathbf{1}^-$ may be unstable even at the electrolysis time scale. The reduction process is assigned to be ruthenium(III)–ruthenium (II) reduction (Eq. (2)).

$$[Ru^{III}(N,O)_2(PPh_3)Cl] + e^- \rightleftharpoons [Ru^{II}(N,O)_2(PPh_3)Cl]^- \quad (2)$$
$$\mathbf{1} \qquad\qquad \mathbf{1}^-$$

The complexes of type **2** display one oxidative and one reductive quasi-reversible responses in the ranges $0.75 \rightarrow 0.87$ V and $-0.43 \rightarrow -0.60$ V, respectively. The one-electron nature of each of the couples is confirmed with the help of constant potential coulometry (Table 3). The responses at positive and negative potentials are respectively assigned to ruthenium(III)–ruthenium(IV) and ruthenium(III)–ruthenium(II) couples, as in Eqs. (3) and (4). The coulometrically generated oxidized ($\mathbf{2}^+$) and reduced ($\mathbf{2}^-$) species are not stable at room temperature.

$$[Ru^{IV}(C,N,O)(PPh_3)(CH_3OH)Cl] + e^- \rightleftharpoons [Ru^{III}(C,N,O)_2(PPh_3)(CH_3OH)Cl]^- \quad (3)$$
$$\mathbf{2}^+ \qquad\qquad \mathbf{2}$$

$$[Ru^{III}(C,N,O)_2(PPh_3)(CH_3OH)Cl] + e^- \rightleftharpoons [Ru^{II}(C,N,O)_2(PPh_3)(CH_3OH)Cl]^- \quad (4)$$
$$\mathbf{2} \qquad\qquad \mathbf{2}^-$$

Here for all the complexes (**1** and **2**) the separation in potential between the two successive redox processes [Eqs. (1)/(2) and Eqs. (3)/(4)] is found to be around 1.3 V, which is in good agreement with the earlier observed average potential difference between the Ru^{IV}/Ru^{III}–Ru^{III}/Ru^{II} couples (1.3–1.5 V) in mononuclear ruthenium complexes having C, N, O, S, SR donor centers [31,34,35,42,44,49].

The reduction potentials are sensitive to the nature of the substituents present in the ligand frame. The plot of E^0_{298} vs. σ_R is linear (Fig. 5), where σ_R in the Hammett constant of the substituents R.

The coordination of the phenolato function in the complexes possibly plays a crucial role to bring down the ruthenium(III)–ruthenium(II) potential as low as

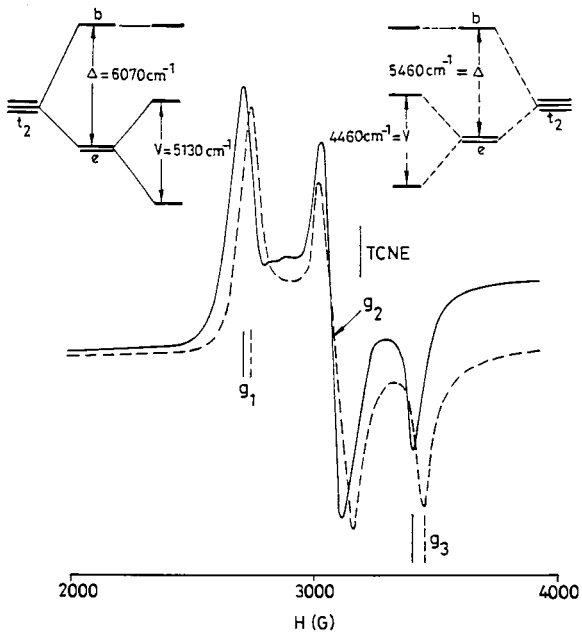

Fig. 3. X-band EPR spectra and t_2 splittings of $Ru^{III}(HL^1)_2(PPh_3)Cl$, **1a** (—) and $Ru^{III}(L^1)(PPh_3)(CH_3OH)Cl$, **2a** (---) in chloroform–toluene (1:1) glass at 77 K.

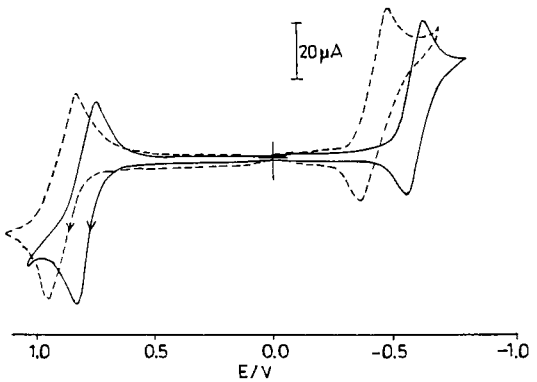

Fig. 4. Cyclic voltammograms of $Ru^{III}(HL^1)_2(PPh_3)Cl$, **1a** (—) and $Ru^{III}(L^5)(PPh_3)(CH_3OH)Cl$, **2e** (---) in dichloromethane.

~ -0.5 V. The low ruthenium(III)–ruthenium (II) potential (~ -0.5 V) might be responsible for the stabilization of the complexes preferentially in the $+3$ state. The bivalent species if formed as an initial product might be oxidized by aerial oxygen.

3. Conclusions

We have observed ruthenium-mediated selective and facile activation of the *ortho*-C–H bond of the pendant phenyl ring of the ligand H_2L, which in turn leads to the formation of stable cyclometallated complexes **2**. The presence of coordinated phenolato oxygen function in combination with metal–carbon σ bond in the complexes **2** preferentially stabilizes the ruthenium ion in the paramagnetic trivalent state.

4. Experimental

The starting complex **A** was prepared according to the reported procedure [36]. The ligands H_2L^1–H_2L^5 were synthesized by condensing salicylaldehyde with the appropriate amines in methanol solvent. Other chemicals and solvents were reagent grade and used as received. Silica gel (60–120 mesh) used for chromatography was purchased from S.D. Fine Chemicals, Bombay, India. For spectroscopic and electrochemical studies HPLC grade solvents were used. Commercial tetraethyl ammonium bromide was converted to pure tetraethyl ammonium perchlorate (TEAP) by following an available procedure [50].

Solution electrical conductivity was checked using a Systronic 305 digital conductivity-bridge. Electronic spectra (700–200 nm) were recorded using a Shimadzu UV 265 spectrophotometer. Near-IR spectra were recorded by using a Hitachi 330 spectrophotometer. Infrared (4000–400 cm^{-1}) spectra were taken on a Nicolet spectrophotometer with samples prepared as KBr pellets. ^1H- and ^{31}P-NMR specta were checked with the use of a 300 MHz Varian FT-NMR spectrometer. Electrochemical measurements were carried out using a PAR model 273A potentiostat/galvanostat. A platinum wire working electrode, a platinum wire auxiliary electrode and Ag/AgCl reference electrode were used in a three-electrode configuration. TEAP was the supporting electrolyte and the solute concentration was $\sim 10^{-3}$ M. The half-wave potential E°_{298} was set equal to 0.5 ($E_{pa} + E_{pc}$), where E_{pa} and E_{pc} are anodic and cathodic cyclic voltammetric peak potentials, respectively. The scan rate used was 50 mV s^{-1}. A platinum wire gauze working electrode was used in coulometric experiments.

Table 3
Electrochemical data at 298 K [a]

Compound	Ru^{IV}–Ru^{III} couple			Ru^{III}–Ru^{II} couple		
	E^0_{298} (V)	(ΔE_p/mV)	n_1 [b]	E^0_{298} (V)	(ΔE_p/mV)	n_2 [c]
1a	0.77	(100)	0.97	−0.58	(90)	–
1b	0.79	(99)	1.02	−0.56	(95)	–
1c	0.81	(98)	0.99	−0.54	(100)	–
1d	0.83	(100)	1.05	−0.52	(100)	–
1e	0.88	(100)	0.95	−0.49	(85)	–
2a	0.75	(90)	0.97	−0.59	(95)	1.08
2b	0.76	(95)	0.98	−0.57	(97)	1.03
2c	0.79	(97)	1.07	−0.52	(90)	0.94
2d	0.82	(100)	1.09	−0.49	(95)	0.97
2e	0.87	(90)	0.94	−0.42	(100)	0.96

[a] Condition: solvent, dichloromethane; supporting electrolyte, TEAP; reference electrode Ag/AgCl; solute concentration, $\sim 10^{-3}$ M; working electrode, platinum wire.

[b] $n_1 = Q/Q'$ where Q' is the calculated coulomb count for $1e^-$ transfer and Q is the columb count found after exhaustive coulometric oxidation at $+1.0$ V.

[c] $n_1 = Q/Q'$ where Q' is the calculated coulomb count for $1e^-$ transfer and Q is the columb count found after exhaustive coulometric reduction at -0.7 V.

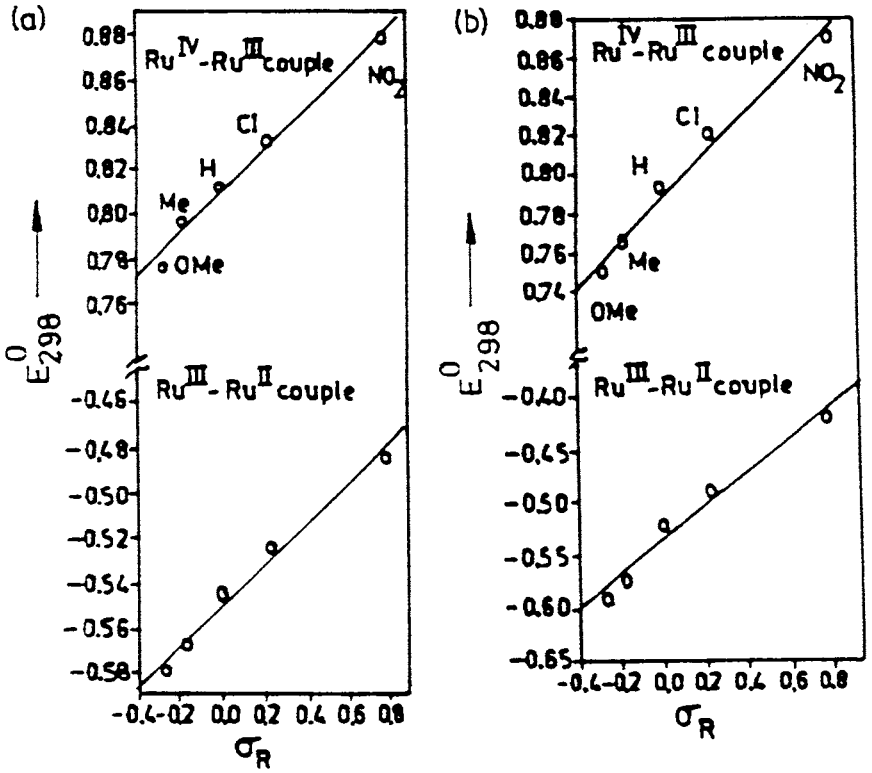

Fig. 5. Least-squares fit of E^0_{298} vs σ_R of (a) $Ru^{III}(HL)_2(PPh_3)Cl$, **1** and $Ru^{III}(L)(PPh_3)(CH_3OH)Cl$, **2**.

All experiments were carried out under dinitrogen atmosphere and are uncorrected for junction potentials. The magnetic susceptibilities were measured on a PAR 155 vibrating-sample magnetometer. EPR measurements were made with a Varian model 109 E-line X-band spectrometer fitted with a quartz dewar for measurements at 77 K (liquid nitrogen). The spectra were calibrated by using radical anion of tetracyanoethylene (TCNE) ($g = 2.0037$). The elemental analyses were carried out with a Carlo Eraba (Italy) elemental analyzer. TGA–DTA experiments were performed by using a Dupont 9900 machine. The FAB mass spectra were recorded on a Jeol SX 102/DA-6000 mass spectrometer. The following Hammett σ values for *para* substituents were used: H, 0.00; Me, -0.17; OMe, -0.27, Cl, $+0.23$; NO_2, $+0.78$ [51].

4.1. Treatment of EPR data

An outline of the procedure can be found in our recent publications [33–35,37–39,42–44]. We note that a second solution also exists that is different from the chosen one, having small distortions and v_1, v_2 values. The experimentally observed near-IR results clearly eliminate the solution as unacceptable.

4.2. Synthesis

Complexes (**1** and **2**) were prepared by following a general method. Details are given for complexes **1a** and **2a**.

4.2.1. Bis-(N-phenylsalicylaldiminato)(triphenylphosphine)(chloro) ruthenium(III) (1a) and (N-phenylsalicylaldiminato)(triphenylphosphine) (chloro) (methanol) ruthenium(III) (2a)

The diruthenium starting complex $[Ru^{II}(CS)(PPh_3)_2Cl_2]_2$ **A** (200 mg, 0.135 mmol) and the ligand H_2L^1 (135 mg, 0.685 mmol) were dissolved in 25 ml of methanol. The resulting mixture was heated to reflux for a period of 5 h. The initial reddish–brown solution was gradually turned to green color. The progress of the reaction was monitored periodically by TLC. The solvent was removed under reduced pressure. The crude product was then purified by column chromatography on a Silica gel (60–120 mesh) column. Unreacted excess ligand was eluted first with benzene and was rejected. The pure bluish–green colored complex **1a** was eluted with chloroform. The yellowish–green complex **2a** was eluted next with 10:1 ratio of chloroform and methanol solvents. On removal of the solvents under reduced pressure the complexes (**1a** and **2a**) were obtained in the

solid state. The complexes were further purified by recrystallization from dichloromethane–hexane (1:5). Yield: 64 mg, 30% for **1a** and 68 mg, 40% for **2a.**

Acknowledgements

Financial support received from the Department of Science and Technology, New Delhi, India, is gratefully acknowledged. Special acknowledgement is made to the Regional Sophisticated Instrumentation Center (RSIC), Indian Institute of Technology, Bombay, for providing NMR and EPR facilities and RSIC, Central Drug Research Institute, Lucknow, for providing the FAB mass spectra.

References

[1] M.A. Bennett, M.I. Bruce, T.W. Matheson, in: G. Wilkinson, F.G.A. Stone, E.W. Ebel (Eds.), Comprehensive Organometallic Chemistry, Pergamon, Oxford, 1982, p. 691.
[2] G.B. Jameson, A. Muster, S.D. Robinson, J.N. Wingfield, J.A. Ibers, Inorg. Chem. 20 (1981) 2448.
[3] J.M. Patric, A.H. White, M.I. Bruce, M.J. Beatson, D.S.C. Black, G.B. Deacon, N.C. Thomas, J. Chem. Soc. Dalton Trans. (1983) 2121.
[4] P. Reveco, R.H. Schmehl, W.R. Cherry, F.R. Fronezek, J. Selbin, Inorg. Chem. 24 (1985) 4078.
[5] M. Nouoyama, Inorg. Chim. Acta 115 (1986) 169.
[6] M.F. McGuiggan, L.H. Pignolet, Inorg. Chem. 21 (1982) 2523.
[7] D.R. Saunders, R.J. Mawby, J. Chem. Soc. Dalton Trans. (1984) 2133.
[8] S. Gopinathan, K. Joseph, C. Gopinathan, J. Organomet. Chem. 269 (1984) 273.
[9] M.I. Bruce, D.N. Duffy, M.G. Humphery, A.G. Swincer, J. Organomet. Chem. 285 (1985) 383.
[10] M.F. Garbukas, J.S. Kasper, L.N. Lewis, J. Organomet. Chem. 276 (1984) 241.
[11] R.O. Rosete, D.J. Cole-Hamilton, G. Wilkinson, J. Chem. Soc. Dalton Trans. (1984) 2067.
[12] L.N. Lewis, J. Am. Chem. Soc. 108 (1986) 743.
[13] L.N. Lewis, J.F. Smith, J. Am. Chem. Soc. 108 (1986) 2728.
[14] L.N. Lewis, Inorg. Chem. 24 (1985) 4433.
[15] N. Bag, S.B. Choudhury, G.K. Lahiri, A. Chakravorty, J. Chem. Soc. Chem. Commun. (1990) 1626.
[16] N. Bag, S.B. Choudhury, A. Pramanik, G.K. Lahiri, A. Chakravorty, Inorg. Chem. 29 (1990) 5014.
[17] E.C. Constable, R.P.G. Henney, D.A. Tocher, J. Chem. Soc. Dalton Trans. (1991) 2335.
[18] E.A. Seddon, K.R. Seddon, The Chemistry of Ruthenium, Elsevier, Amsterdam, 1984.
[19] T.A. Stephenson, G. Wilkinson, J. Inorg. Nucl. Chem. 28 (1966) 945.
[20] J.V. Kingston, G. Wilkinson, J. Inorg. Nucl. Chem. 28 (1966) 2709.
[21] J. Halpern, B.R. James, A.L.W. Kemp, J. Am. Chem. Soc. 88 (1966) 5142.
[22] R. Colton, R.H. Farthing, Aust. J. Chem. 24 (1971) 903.
[23] M.L. Berch, A. Davison, J. Inorg. Nucl. Chem. 35 (1973) 3763.
[24] A.J. Hewitt, J.H. Holloway, R.D.Peacock, J.B. Raynor, I.L. Wilson, J. Chem. Soc. Dalton Trans. (1976) 579.
[25] L.H. Pignolet, S.H. Wheeler, Inorg. Chem. 19 (1980) 935.
[26] M.M. Taquikhan, D. Srinivas, R.I. Kureshy, N.H. Khan, Inorg. Chem. 29 (1990) 2320.
[27] M. Ke, S.J. Rettig, B.R. James, D. Dolphin, J. Chem. Soc. Chem. Commun. (1987) 1110.
[28] J.W. Seyler, C.R. Leidner, Inorg. Chem. 29 (1990) 3636.
[29] M. Ke, C. Sistha, B.R. James, D. Dolphin, J.W. Sarapany, J.A. Ibers, Inorg. Chem. 30 (1991) 4776.
[30] M. Beley, J. Collin, R. Louis, B. Metz, J. Sauvage, J. Am. Chem. Soc. 113 (1991) 8521.
[31] G.K. Lahiri, S. Bhattacharya, M. Mukherjee, A.K. Mukherjee, A. Chakravorty, Inorg. Chem. 26 (1987) 3359.
[32] J.D. Gilbert, D. Rose, G. Wilkinson, J. Chem. Soc. A (1970) 2765.
[33] A.K. Mahaparta, S. Datta, S. Goswami, M. Mukherjee, A.K. Mukherjee, A. Chakravorty, Inorg. Chem. 25 (1986) 1715.
[34] P. Ghosh, A. Pramanik, N. Bag, G.K. Lahiri, A. Chakravorty, J. Organomet. Chem. 454 (1993) 237.
[35] P. Munshi, R. Samanta, G.K. Lahiri, Polyhedron 17 (1998) 1913.
[36] J.D. Gilbert, M.C. Baird, G. Wilkinson, J. Chem. Soc. A (1968) 2198.
[37] R. Hariram, B.K. Santra, G.K. Lahiri, J. Organomet. Chem. 540 (1997) 155.
[38] G.K. Lahiri, S. Bhattacharya, B.K. Ghosh, A. Chakravorty, Inorg. Chem. 26 (1987) 4324.
[39] A. Pramanik, N. Bag, G.K. Lahiri, A. Chakravorty, J. Chem. Soc. Dalton Trans. (1990) 3823.
[40] G.M. Bryant, J.E. Fergusson, H.K.J. Powell, Aust. J. Chem. 24 (1971) 257.
[41] A. Ceulemans, L.G. Vanquickborne, J. Am. Chem. Soc. 103 (1981) 2238.
[42] N. Bag, G.K. Lahiri, S. Bhattacharya, L.R. Falvello, A. Chakravorty, Inorg. Chem. 27 (1988) 4396.
[43] A. Pramanik, N. Bag, D. Ray, G.K. Lahiri, A. Chakravorty, Inorg. Chem. 30 (1991) 410.
[44] S. Chattopadhyay, N. Bag, P. Basu, G.K. Lahiri, A. Chakravorty, J. Chem. Soc. Dalton Trans. (1990) 3389.
[45] B. Bleaney, M.C.M. O'Brein, Proc. Phys. Soc. London Sect B 69 (1956) 1216.
[46] J.S. Griffith, The Theory of Transition Metal Ions, Cambridge University Press, London, 1961, p. 364.
[47] N.J. Hill, J. Chem. Soc. Faraday Trans. 2 (1972) 427.
[48] C. Daul, A. Goursot, Inorg. Chem. 24 (1985) 3554.
[49] B.M. Holligan, J.C. Jeffery, M.K. Norgett, E. Schatz, M.D. Ward, J. Chem. Soc. Dalton Trans. (1992) 3345.
[50] D.T. Sawyer, A. Sobkowiak, J.L. Roberts Jr., Experimental Electrochemistry for Chemists, 2nd edn, Wiley, New York, 1995.
[51] L.P. Hammett, Physical Organic Chemistry, 2nd edn, McGraw–Hill, NewYork, 1970.